ORIGINAL

Heat transfer improvement in simulated small battery compartment using metal oxide (CuO)/deionized water nanofluid

N. Ahmed Bin-Abdun[1,2] · Z. M. Razlan[1] · S. A. Bakar[1] · C. H. Voon[3] · Z. Ibrahim[1] · W. K. Wan[1] · M. J. M. Ridzuan[1]

Abstract

Improving the heat transfer coefficient of working fluids is essential for achieving the best performance of manufacturing systems. As a replacement of conventional working fluids, nanofluids have a high potential for improving this heat transfer coefficient. However, nanofluids are seldom implemented in actual systems, and several factors should be considered before actual application. Accordingly, this study investigated the thermophysical properties and heat transfer rate of CuO/deionized water nanofluid with and without sodium dodecyl sulfate (SDS) surfactants. Three different volumetric concentrations of the nanofluid were prepared using a two-step preparation method. The experimental steps were divided into two phases: static and dynamic. In these experiments, the thermophysical properties of the prepared nanofluids and the heat transfer coefficient were measured using an apparatus designed based on an actual heat exchanger for a lithium ion polymer battery compartment. The effects of flow rate and surfactants on the heat transfer rate of the nanofluids with varying volumetric concentrations of 0.08%, 0.16%, and 0.40% were analyzed. The results indicate that the heat transfer rate increases considerably as the flow rate increases from 0.5 L/min to 1.2 L/min and with the presence of surfactants. The highest heat transfer rate was obtained at a 0.40% volumetric concentration of CuO/deionized water nanofluid with SDS surfactant.

Keywords Nanofluid · SDS surfactant · Small space · Heat transfer rate

1 Introduction

Improvements in the heat transfer performance are required for various applications in engineering [1, 2]; however, this has been an enormous challenge [3]. For this purpose, nanofluids have shown promising potential as a superior alternative to traditional fluids. Nanofluids are an extension of ordinary working fluids (e.g., ethylene glycol and water) that have added solid particles ($1 \approx 100$ nm) in the form of metals oxides, carbides, carbon nanotubes, or ceramics. Nanofluids

✉ Z. M. Razlan
zuradzman@unimap.edu.my

1 School of Mechatronic Engineering, Universiti Malaysia Perlis, Pauh Putra Campus, 02600 Arau, Perlis, Malaysia

2 Department Air-Conditioning, Seiyun Community College, Hadhramoot, Yemen

3 Institute of Nano Electronic Engineering, Universiti Malaysia Perlis, Seriab, 01000 Kangar, Perlis, Malaysia

exhibit better heat transfer rates, even at small concentrations of nanoparticles than ordinary working fluids [4, 5]. However, numerous criteria such as the maintenance and lifespan of supporting instruments, e.g., pumps, should be taken into consideration. Several experimental studies on replacing ordinary working fluids, i.e., water and coolant, by nanofluids, and the impact of using nanofluids in systems have been conducted. Some promising applications of nanofluids are in solar collectors, refrigerators, heat exchangers, etc.

Recently, several studies have experimentally and theoretically investigated the properties and characteristics of nanofluids. From the available literature, it can be concluded that the improvement in the heat transfer rate of nanofluids depends on certain factors such as temperature, particle volume concentration, shape and size of the nanoparticles, and the heat transfer properties of the base fluids [6, 7]. However, the development of nanofluid technology is hindered by several challenges: stability issues, requirements for higher pumping power owing to increased viscosity, and high cost of synthesizing nanoparticles [8, 9]. Another challenge facing nanofluid applications is the erosion of oxide nanoparticles on the pipes [10, 11].

The influence of oxide nanoparticles on the thermal conductivity of a nanofluid has been studied by several researchers [12, 13]. Studies have shown that the thermal conductivity of the nanofluid can be improved up to 60% with an increase in the volume concentration of nanoparticles. This is mainly owing to the influence of their thermophysical properties [14, 5].

This study investigated the application of selected nanofluids; specifically, CuO/deionized water in an environment similar to that of actual heat exchangers in a lithium polymer (LiPO) battery compartment. Considering safety precautions, the heat load from the battery was simulated using a stainless steel water tank, through which the working fluid, isothermal water, flows to maintain the heat load generated from the actual battery. The analysis results and conclusions drawn herein can form the basis of cooling system designs for battery compartments that have conditions similar to those considered in this study.

2 Experimental setup and methodology

2.1 Materials

In this study, CuO particles developed by US Research Nanomaterials, Inc., were used. The properties of the nanoparticles are given in Table 1 (US Research Nanomaterials, Inc.). Deionized water was used as the base fluid, and it was deeply demineralized, ultrapure water.

Scanning electron microscopy (SEM) analysis (LV mode (4.0 nm, 20 kV)) was performed on dried nanoparticles to describe the size of the CuO nanoparticles and their morphology (Fig. 1). The SEM results showed that CuO nanoparticles have a (virtually) spherical shape and their average diameter is 70–78 nm.

2.2 Instruments

2.2.1 Nanofluid preparation

A two-step method was used in the preparation. First, the nanoparticles were dispersed in deionized water (1 L) with constant stirring for 3 h by a magnetic stirrer (MSH-30D) (950 rpm, 30 °C). Ultrasonication (DC200H) was conducted

Table 1 Properties of CuO nanoparticles

Color	Black
Morphology	Nearly spherical
Size	80 nm
Thermal conductivity, W/m. K	20
True density, kg/m^3	6400
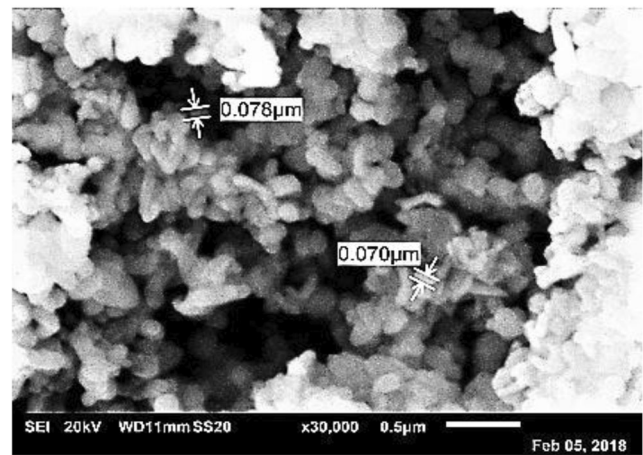
CuO 80nm P03 x30k

Fig. 1 SEM images of CuO nanoparticles

for 12 h to eliminate any agglomerations in the nanofluid with proper suspension in deionized water to ensure that there were no collisions among particles. The nanofluid was stabilized by the addition of sodium dodecyl sulfate (SDS). In this study, the nanofluid was prepared with 0.08%, 0.16%, and 0.40% volume concentrations of nanoparticles in deionized water; the volume concentration was calculated using the following relation (law of mixture) [15, 16]:

$$\%\text{Volume Concentration}, \varphi = \frac{\left(\dfrac{m_{np}}{\rho_{np}}\right)}{\left(\dfrac{m_{np}}{\rho_{np}} + \dfrac{m_{bf}}{\rho_{bf}}\right)} \qquad (1)$$

where m is mass, ρ density, and the subscripts np and bf signify nanoparticle and base fluid, respectively. Note that the mass of the nanoparticles was measured using a precision analytical balance (Model B-220C). Finally, the nanofluids were observed for 96 h to ensure that sedimentation did not occur (Fig. 2).

2.2.2 Measurement of thermophysical properties

A thermal property analyzer (KD2 Pro) was used to quantitatively measure the thermal conductivity of the nanofluid. The accuracy of the thermal property analyzer (KD2 Pro) is ±0.5%. By using a temperature controller unit (water bath), the temperature of the nanofluid sample was stabilized during the measurement of thermal conductivity. The accuracy of KD2 Pro was calibrated using glycerin to verify the performance of the KS-1 sensor for water. The standard values were compared with the obtained thermal conductivity values of water. As shown in Fig. 3, the values obtained were consistent with the standard values, and the maximum uncertainty was estimated to be 6%.

Fig. 2 Stability of CuO/deionized water nanofluid (with surfactant)

The viscosity of the nanofluid was measured using a viscometer (model LVDV-Pro, Brookfield Instruments) with an accuracy of ±1.0%. Differential scanning calorimetry (DSC) was used to measure the specific heat of the nanofluid. The accuracy of the DSC for heat and temperature of sample measurement was ±1.0% and ± 0.01% °C, respectively.

2.2.3 Experimental rigs

Figure 4 shows a schematic diagram of the experimental setup used to measure the heat transfer rate of each test condition shown in Table 2.
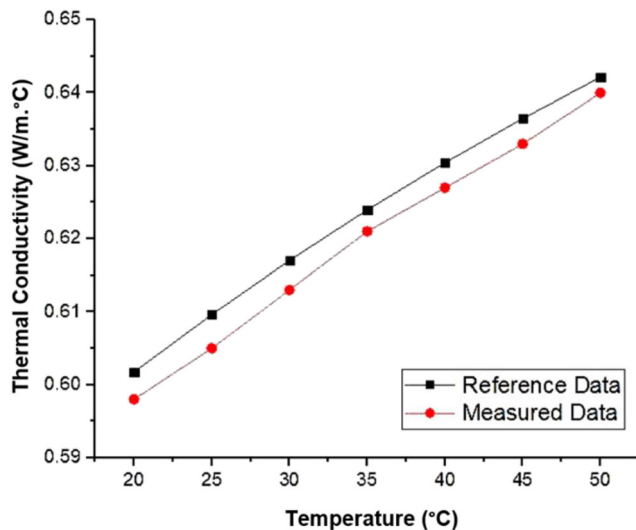

Fig. 3 Comparison of measured thermal conductivity of distilled water with reference data

The experimental setup consists of three separated cycles, i.e., the main cycle using the nanofluid and the other two using water. For the main cycle, one liter of the nanofluid (CuO/ deionized water) is contained in the nanofluid tank. In the main cycle, the nanofluid flows from the nanofluid tank to the heat exchanger using the pump and then flows back to the nanofluid tank. The flow is controlled by a gate valve and monitored with a flow meter. The secondary cycle is used to control the temperature of the nanofluid in the nanofluid tank to match the desired inlet temperature (20 ± 0.5 °C) of the heat exchanger. With water as the working fluid, the cooling coil temperature inside the nanofluid tank is controlled by cooling the water with Temperature Bath 1. A stainless steel water tank is used as the heat source for this experiment, replacing the actual selected LiPO battery. The surface temperature is measured and the heat load is controlled to the desired value using Temperature Bath 2, i.e., the third cycle. In this experiment, the heat load could be controlled and kept constant at 82 W via the constant flow rate at a constant temperature of Temperature Bath 2, replicating the heat load of the selected LiPO battery. Conversely, the surface temperature of the stainless steel water tank shall vary according to the changes in the cooling load of the heat exchanger due to changes in the flow rate and volumetric concentration of the nanofluid. A 50 mm thick polystyrene foam covers the compartment containing the stainless steel water tank and the heat exchanger to ensure no heat is released outside the compartment. The test compartment is shown in more detail in Fig. 5.

The nanofluid tank dimensions are ($L \times W \times H$) 200 mm × 125 mm × 60 mm. The required flow rate of the nanofluid is transferred to the flow meter using the gate valve RMB-SSV,

Fig. 4 Schematic diagram of the experimental setup
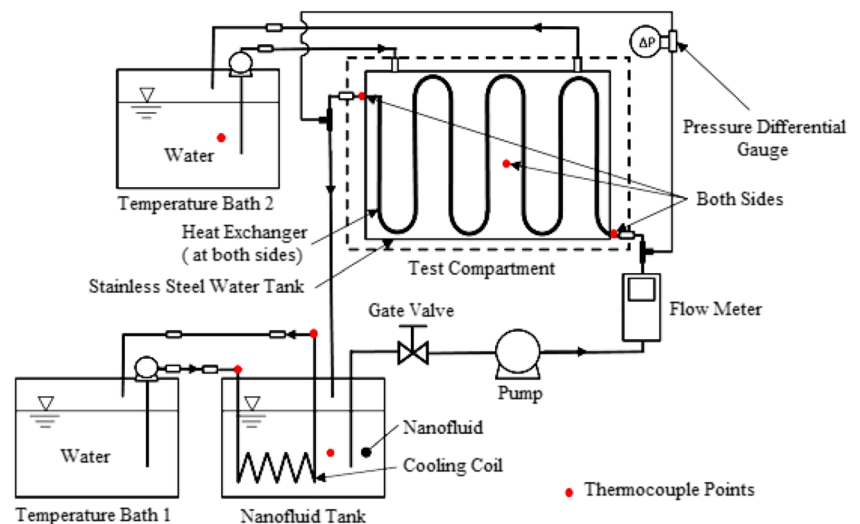
with a temperature limit of 54 °C and a pressure limit of 100 psi. The flowmeter comprises a precision metering valve with reading accuracy ±0.3%. The heat exchanger consists of two helical tubes made from copper (dimensions, OD × L: ϕ 6.35 mm × 2200 mm) with a thickness of 0.7 ± 0.02 mm, roughness 0.0013–0.0015 mm. The heating system (Temperature Bath 2) uses a heater (Omega HCTB-3020-240 V) with a temperature range of −40 to 200 °C and with a built-in temperature controller with accuracy ±1 °C. The heater is dipped into the tank (8 L) to ensure that water at a constant temperature flows into the stainless steel water tank as the heat load of the test compartment. Furthermore, in order to minimize temperature loss to the surroundings, all tube parts are isolated. The inlet temperature requirement (40 °C) of the stainless steel water tank is set at the heater temperature controller. The stainless steel water tank dimensions are (L × W × H) 350 mm × 50 mm × 260 mm. Thermocouples (K-type) with an accuracy of ±0.1 °C of the full scale are installed at the inlet and outlet of the heat exchanger for measuring the bulk temperature of the nanofluid and the temperatures inside the nanofluid tank, on the surface of the stainless steel water tank, at the inlet and outlet of the cooling coil from Temperature Bath 1, and inside Temperature Bath 2. These locations are indicated by red dots in Fig. 4. The data acquisition system (Agilent 34970A) is used to measure the temperature from each thermocouple, which can be displayed up to three decimal places. A differential pressure gauge is fitted across the test sections, i.e., the heat exchanger, to measure the pressure

drop along the heat exchanger copper tube. All of the equipment used in the system are manufacturer-calibrated and can be cleaned easily.

Through initial examination, it was found that the system requires 140–180 min to reach the steady state condition. The readings were taken after the system attained steady state. Each measurement was repeated twice. The essential parameters measured in the experiment were flow rate, temperatures (as described in the previous paragraph), and the pressure drops of the working fluids along the heat exchanger.

3 Method

Volumetric flow rates, inlet and outlet temperatures of the heat exchanger in the test compartment, and temperature of the cooling coils (helical tubes) were collected during the experiment as references to analyze the effect of surfactant concentrations. The selected performance indicators were thermophysical properties, measured heat transfer, and convective heat transfer coefficient. All these indicators were produced using equations presented in this section. To determine the different thermophysical properties of the nanofluid, the bulk temperature is used, i.e., the average of the outlet and inlet temperatures of the heat exchanger.

The equation of Yu and Choi [17] is used in calculating the thermal conductivity of nanofluids:

$$k_{nf} = \left(\frac{k_{np} + 2k_{bf} + 2\left(k_{np}-k_{bf}\right)(1+\beta)^3 \varphi}{k_{np} + 2k_{bf} - 2\left(k_{np}-k_{bf}\right)(1+\beta)^3 \varphi} \right) k_{bf}, (\beta = 0.1)$$

When the particle shape is spherical

$$(2)$$

where k is the thermal conductivity, φ is the nanoparticle volume concentration, and the subscripts nf, np, and bf signify nanofluid, nanoparticle, and base fluid, respectively.

Table 2 Volumetric flow rate and volume concentration of CuO/deionized water at heat exchanger

Volume concentration (%)	Volumetric flow rate (L/min)			
0.08	0.5	0.8	1.0	1.2
0.16	0.5	0.8	1.0	1.2
0.40	0.5	0.8	1.0	1.2

Fig. 5 Details of heat exchanger and stainless steel water tank inside test compartment
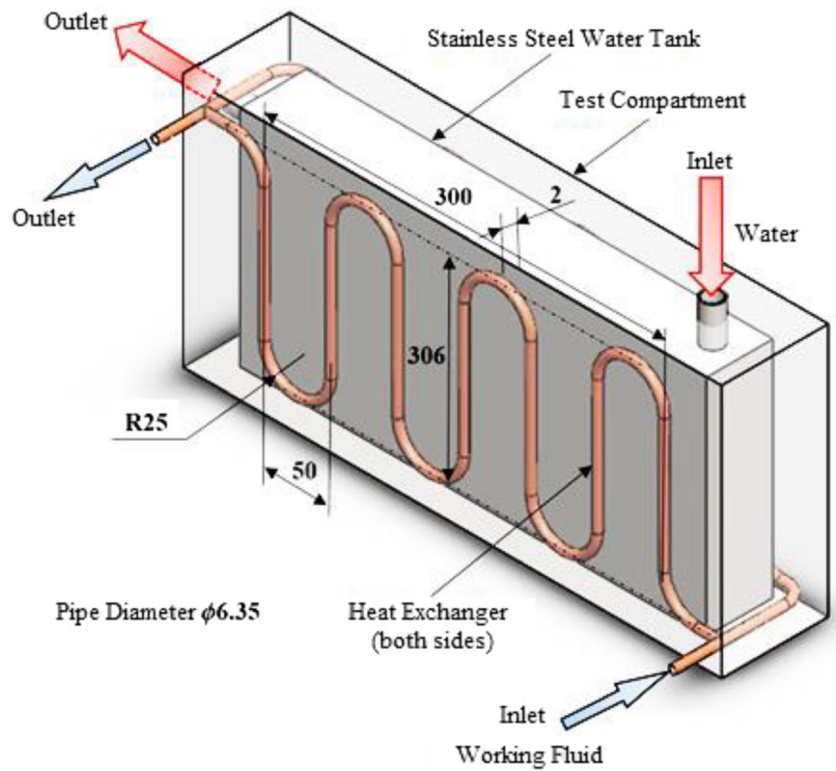
The density and specific heat of the nanofluids can be defined as follows [16, 18]:

$$\rho_{nf} = \varphi\rho_{np} + (1-\varphi)\rho_{bf} \tag{3}$$

$$Cp_{nf} = \frac{\varphi(\rho Cp)_{np} + (1-\varphi)(\rho Cp)_{bf}}{\rho_{nf}} \tag{4}$$

where ρ is density and Cp is specific heat.

The viscosity of the nanofluids is determined using the formula proposed by Einstein (see [19, 20]):

$$\mu_{nf} = (1 + 2.5\varphi)\mu_{bf} \tag{5}$$

where μ_{nf} is the viscosity of the nanofluid and μ_{bf} is the viscosity of the base fluid.

In this study, Eqs. (2) to (5) were used to obtain theoretical data as reference to the experimental data. The results are shown in Fig. 6.

The Reynolds number is defined as follows:

$$Re = \frac{\rho Vd}{\mu} \tag{6}$$

where V is the velocity of the flow, d is the hydraulic diameter of the tubes, and μ is the dynamic viscosity of the fluid.

The Prandtl number is defined as follows:

$$Pr = \frac{\upsilon}{\alpha} = \frac{\mu Cp}{k} \tag{7}$$

where v is kinematic viscosity and α is thermal diffusivity.

The heat transfer rate is calculated from the following formula (see [21]):

$$Q = \dot{m}Cp\Delta T = \dot{m}Cp(T_{out} - T_{in}) \tag{8}$$

where $\dot{m}$ is mass flow rate, T_{in} is the inlet temperature of the cooling coils, and T_{out} is the outlet temperature of the cooling coils.

The heat transfer coefficient is determined by the relation (see [21, 22]),

$$h_{exp.} = \frac{\dot{m}\,Cp(T_{out} - T_{in})}{A_S\Delta T_{lm}} \tag{9}$$

where $h_{exp.}$ is the heat transfer coefficient, A_S is the total peripheral area of the tubes, and ΔT is the logarithm mean temperature difference.

The formula of the peripheral area is given by

$$A = 2\pi dL \tag{10}$$

where L is the length of the tube and d is the diameter of the tube.

The Nusselt number can be defined as follows:

$$Nu_{exp.} = \frac{h_{exp.}\,d}{k} \tag{11}$$

where d is the hydraulic diameter of the tube.

(a) Thermal Conductivity
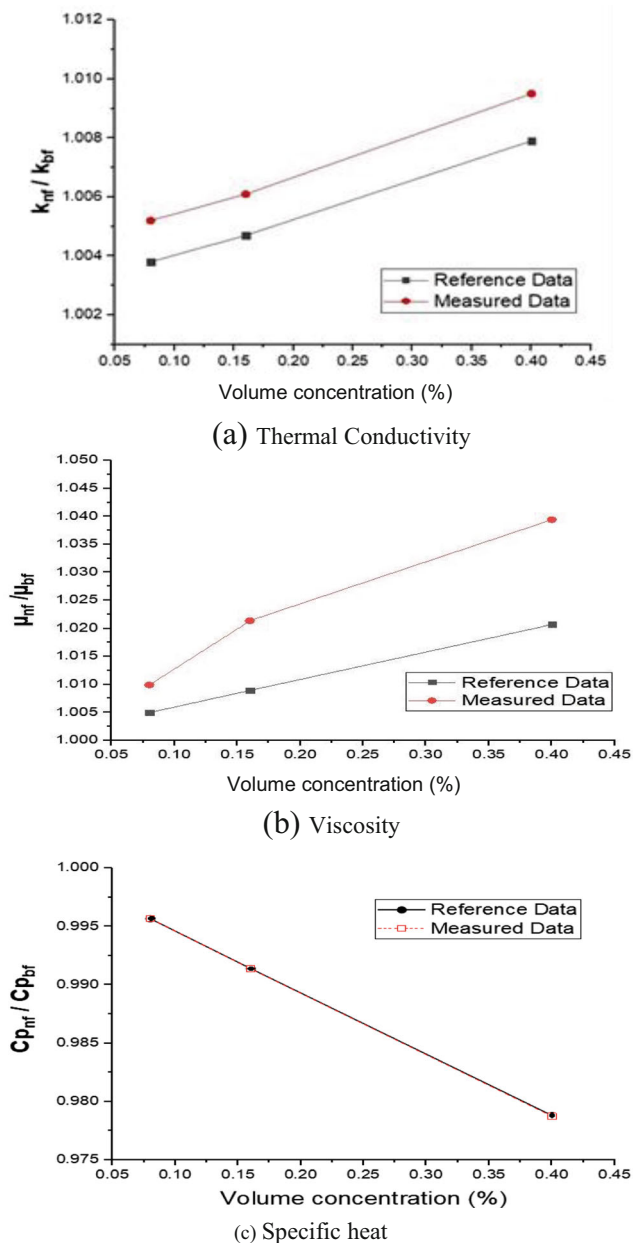

(b) Viscosity

(c) Specific heat

Fig. 6 Thermophysical properties of nanofluid without surfactant vs. volume concentrations

4 Uncertainty analysis

Uncertainty analysis of the experimental data was also conducted for temperature and flow rate measurement of the working fluid, in order to verify the accuracy of the final data (e.g., Reynolds number, average Nusselt number heat transfer coefficient, total heat transfer). The uncertainty analysis was conducted by calculating the deviation of the measurements (Gum Method). The maximum uncertainty values for key thermophysical properties were calculated, i.e., total heat transfer (Q) = 3.1%, Reynolds number (Re) = 1.9%, and heat transfer coefficient (h) = 2.7%. In addition, the uncertainty of the volume concentration was 0.2%, and changes in the flow

rates were found to have a clear effect on uncertainty. The results showed larger uncertainties at lower flow rates, with a maximum uncertainty of 3.0% of the flow rate.

5 Results and discussion

5.1 Thermophysical properties

Figure 6 presents the change in various thermophysical properties with varying volume concentrations of the CuO nanoparticles; in addition, the theoretical data calculated using correlations are compared with the experimentally measured data.

Figure 6a shows that the thermal conductivity of the nanofluid rises when the volume concentration of the nanoparticles inside the deionized water increases. In addition, the results were calculated using the formula of Yu and Choi [23]. The experimental results are similar to that obtained by the Yu and Choi model. The maximum difference between the experimental results and the results of the Yu and Choi model is 0.0016.

The experimentally measured viscosity was compared with that obtained by the Einstein model, as shown in Fig. 6b. Note that the viscosity increases with the volumetric concentration of the nanoparticles.

The experimentally measured specific heat was compared with that obtained by the theoretical formula. Figure 6c shows that the specific heat decreases as the volumetric concentration of the nanoparticles increases.

5.2 Heat transfer rates

The results for heat transfer rates at various flow rates for deionized water and 0.08%, 0.16%, and 0.40% volumetric concentrations of CuO nanoparticles are presented in Fig. 7.
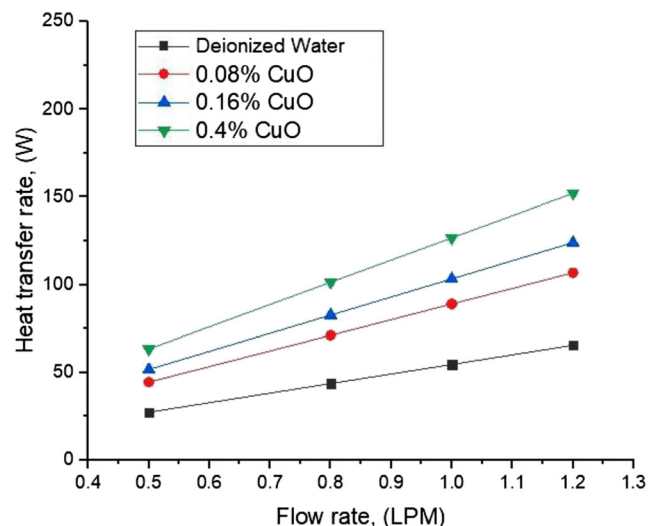

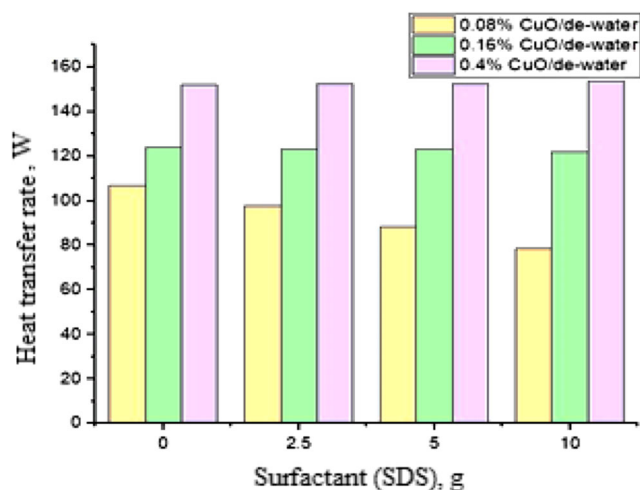**Fig. 7** Heat transfer rate versus flow rate for deionized water and nanofluids

Fig. 8 Effect of surfactant concentrations on heat transfer rate

The values for deionized water were determined as a baseline for measuring the thermal improvement when using nanofluids. In the case of deionized water, the heat transfer rate is 27.3 W at 0.5 L/min and 65.6 W at 1.2 L/min. It can be seen that the heat transfer rates are higher for the nanofluid compared with deionized water. The highest increase in heat transfer is observed at 0.40% volumetric concentration of CuO nanoparticles.

The heat transfer rates for 0.08%, 0.16%, and 0.40% volumetric concentrations of CuO nanoparticles are 16%, 19%, and 23% higher than those of deionized water, respectively.

Figure 8 represents the relationship between heat transfer and adding 2.5 g, 5 g, and 10 g of surfactants to the nanofluids, illustrating the result of surfactant addition on the nanofluid performance. The results show that the heat transfer rate decreases at 0.08% and 0.16% volumetric concentrations as the surfactant concentration is increased, showing a maximum decrease of almost 35% and 1.2%, respectively. This is due to the effect of the surfactant on viscosity. At 0.4% volumetric concentration, the results show a slight increase in the heat transfer rate.

6 Conclusion

This study investigated the convective heat transfer performance of copper cooling coils in small spaces using deionized-water-based CuO nanofluids.

(1) Using CuO/deionized water nanofluid can significantly increase heat transfer rates compared with using only deionized water. For the experimental conditions shown in Table 2, the best heat transfer rate is observed for a flow rate of 1.2 L/min, with an improvement of up to 56% realized using a 0.40% volumetric concentration of nanoparticles.

(2) The results of the experiment show that the improvement in heat transfer rate for nanofluids depends highly on the nanoparticle volume concentration. The test range is from 0.08% to 0.40% volumetric concentration.

(3) Heat transfer rates are found to be weak for high surfactant concentrations.

(4) Increases in surfactant concentrations of 2.5 g, 5 g, and 10 g result in decreases in the heat transfer rate for small volumetric concentrations. It is clear that the improvement in the heat transfer rate depends on finding the ideal proportion of surfactant to nanoparticles present in the nano-mixture.

(5) The higher heat transfer rates obtained using nanofluids instead of traditional fluids demonstrate the high potential of nanofluids to overcome the issue of large thermal emissions in smaller spaces.

References

1. Zangeneh A, Vatani A, Fakhroeian Z, Peyghambarzadeh SM (2016) Experimental study of forced convection and subcooled flow boiling heat transfer in a vertical annulus using different novel functionalized ZnO nanoparticles. Appl Therm Eng 109:789–802. https://doi.org/10.1016/j.applthermaleng.2016.08.056

2. Shahrul IM, Mahbubul IM, Saidur R, Sabri MFM (2016) Experimental investigation on Al_2O_3-W, SiO_2-W and ZnO-W nanofluids and their application in a shell and tube heat exchanger. Int J Heat Mass Transf 97:547–558. https://doi.org/10.1016/j.ijheatmasstransfer.2016.02.016

3. Li Y, Tung S, Schneider E, Xi S (2009) A review on development of nanofluid preparation and characterization. Powder Technol 196: 89–101. https://doi.org/10.1016/j.powtec.2009.07.025

4. Gupta M, Arora N, Kumar R et al (2014) A comprehensive review of experimental investigations of forced convective heat transfer characteristics for various nanofluids. Int J Mech Mater Eng 9(1):11

5. Wang XQ, Mujumdar AS (2007) Heat transfer characteristics of nanofluids: a review. Int J Therm Sci 46:1–19. https://doi.org/10.1016/j.ijthermalsci.2006.06.010

6. Chang M, Liu H, Tai CY (2011) Preparation of copper oxide nanoparticles and its application in nanofluid. Powder Technol 207:378–386. https://doi.org/10.1016/j.powtec.2010.11.022

7. Gangadevi R, Vinayagam BK, Senthilraja S (2018) Effects of sonication time and temperature on thermal conductivity of CuO/water and Al_2O_3/water nanofluids with and without surfactant. Mater Today Proc 5:9004–9011. https://doi.org/10.1016/j.matpr.2017.12.347

8. Saidur R, Leong KY, Mohammad HA (2011) A review on applications and challenges of nanofluids. Renew Sust Energ Rev 15: 1646–1668. https://doi.org/10.1016/j.rser.2010.11.035

9. Abasi B, Dehkordi F, Abdollahi A (2018) Experimental investigation toward obtaining the effect of interfacial solid- liquid interaction and base fluid type on the thermal conductivity of CuO- loaded nanofluids. Int Commun Heat Mass Transfer 97:151–162. https://doi.org/10.1016/j.icheatmasstransfer.2018.08.001

10. Lotfizadehdehkordi B, Kazi SN, Hamdi M et al (2013) Investigation of viscosity and thermal conductivity of alumina nanofluids with addition of SDBS. Heat Mass Transf:1109–1115. https://doi.org/10.1007/s00231-013-1153-8

11. Chakraborty S, Saha SK, Pandey JC, Das S (2011) Experimental characterization of concentration of nanofluid by ultrasonic technique. Powder Technol 210:304–307. https://doi.org/10.1016/j.powtec.2011.03.035

12. Hossein M, Darvanjooghi K, Esfahany MN (2016) Experimental investigation of the effect of nanoparticle size on thermal conductivity of in-situ prepared silica – ethanol nanofluid. Int Commun Heat Mass Transfer 77:148–154. https://doi.org/10.1016/j.icheatmasstransfer.2016.08.001

13. Nanofluid M (2010) Enhanced thermal conductivity of nanofluids: a state-of-the-art review. Microfluid Nanofluid 8:145–170. https://doi.org/10.1007/s10404-009-0524-4

14. Afrand M (2017) Experimental study on thermal conductivity of ethylene glycol containing hybrid nano-additives and development of a new correlation. Appl Therm Eng 110:1111–1119. https://doi.org/10.1016/j.applthermaleng.2016.09.024

15. Zakaria I, Azmi WH, Mohamed WANW et al (2015) Experimental investigation of thermal conductivity and electrical conductivity of Al_2O_3 nanofluid in water - ethylene glycol mixture for proton exchange membrane fuel cell application. Heat Mass Transf 61:61–68. https://doi.org/10.1016/j.icheatmasstransfer.2014.12.015

16. Pak BC, Cho YI (1998) Hydrodynamic and heat transfer study of dispersed fluids with submicron metallic oxide particles. Exp Heat Transfer 11:151–170. https://doi.org/10.1080/08916159808946559

17. Yu W, Choi SUS (2003) The role of interfacial layers in the enhanced thermal conductivity of nanofluids: a renovated Maxwell model. J Nanopart Res 5:167–171

18. Xuan Y, Roetzel W (2000) Conceptions for heat transfer correlation of nanofluids. Int J Heat Mass Transf 43:3701–3707

19. Brady JF (1984) The Einstein viscosity correction in n dimensions. Int J Multiphase Flow 10:113–114

20. Khair AS (2006) The 'Einstein correction' to the bulk viscosity in n dimensions. J Colloid Interface Sci 302:702–703. https://doi.org/10.1016/j.jcis.2006.07.076

21. Pandey SD, Nema VK (2012) Experimental analysis of heat transfer and friction factor of nanofluid as a coolant in a corrugated plate heat exchanger. Exp Thermal Fluid Sci 38:248–256. https://doi.org/10.1016/j.expthermflusci.2011.12.013

22. Leong KY, Saidur R, Khairulmaini M et al (2012) Heat transfer and entropy analysis of three different types of heat exchangers operated with nanofluids. Int Commun Heat Mass Transfer 39:838–843. https://doi.org/10.1016/j.icheatmasstransfer.2012.04.003

23. Ho CJ, Chen WC (2013) An experimental study on thermal performance of Al_2O_3/water nanofluid in a minichannel heat sink. Appl Therm Eng 50:516–522. https://doi.org/10.1016/j.applthermaleng.2012.07.037